Rapid and sensitive time-resolved fluorescence immunochromatographic strip for detecting H10 subtype avian influenza virus

Ping Wang , Han Wu , Jiamin Fu , Jun Zhang , Linfang Cheng , Fumin Liu , Hangping Yao , Nanping Wu , Haibo Wu *

State Key Laboratory for Diagnosis and Treatment of Infectious Diseases, National Clinical Research Center for Infectious Diseases, the First Affiliated Hospital, School of Medicine, Zhejiang University, Hangzhou 310003, China

ABSTRACT

Human infections with the H10 subtype avian influenza virus (AIV) have been reported in recent years, raising concern about potential human-to-human transmission. Effective field detection methods are essential for monitoring and controlling the spread of this virus. The objective of this study was to develop a rapid, highly sensitive, and specific detection system for the H10 subtype AIV. Two monoclonal antibodies targeting the hemagglutinin (HA) protein of H10 AIV were generated and characterized. One antibody was conjugated to europium-chelate fluorescent nanospheres and used as a tracer, while the other was immobilized on the test line to capture antigen. A time-resolved fluorescence immunochromatographic strip was then constructed and evaluated for analytical performance. The assay achieved a detection limit of 0.015 hemagglutination units for virus-containing allantoic fluid and 1.1 ng/mL for purified HA protein, which represents a substantial improvement in sensitivity compared with conventional immunochromatographic assays. The test correctly identified all H10 subtype strains examined, including H10N2, H10N3, H10N5, H10N7, and H10N8, and showed no cross-reactivity with nine other subtype AIVs or seven non-influenza avian pathogens. Reproducibility was high, with relative standard deviations below 10% across repeated assays. Receiver operating characteristic analysis yielded areas under the curve of 0.9896 and 0.9722 for virus- and protein-based evaluations, respectively, confirming excellent diagnostic accuracy. Field evaluation with 174 avian samples, including cloacal swabs, throat swabs, and fecal samples, demonstrated 100% concordance with real-time polymerase chain reaction. The entire test procedure was completed within 15 minutes, requiring minimal equipment and technical expertise. In conclusion, the developed time-resolved fluorescence immunochromatographic strip provides a rapid, sensitive, and highly specific tool for detecting the H10 subtype AIV. Its superior performance and ease of use make it well suited for routine surveillance and early warning in poultry farms and live bird markets, thereby supporting disease control and protecting public health.

Introduction

Avian influenza viruses (AIVs) infect a wide range of avian species, including poultry, seabirds, and waterfowl, and can cause systemic or respiratory disease. Genetic mutations also enable cross-species transmission to mammals such as swine, canines, and humans, resulting in serious economic losses and posing a significant public health threat (Kang et al., 2024; Postel et al., 2025). The H10 subtype AIV is generally classified as a low-pathogenic virus, and phylogenetic analyses indicate that its genes fall into two major lineages, North American and Eurasian. In birds, H10 viruses typically cause no or only mild symptoms, making their spread easy to overlook (Liu et al., 2009; Bi et al., 2024). However, birds are not the only hosts of this virus. In Guangdong Province, China, an H10N8 strain circulating in live-poultry markets was found to have infected stray dogs (Su et al., 2014). In addition, mass mortality events among seals caused by H10N7 virus infection have been reported in Denmark, Sweden, Germany, and the Netherlands (Krog et al., 2015; Zohari et al., 2014).

Several cases of human infection, including fatalities, have also been documented, all linked to exposure in live-poultry markets. In 2004, two infants in Egypt were infected with H10N7 virus (Herfst et al., 2020), followed in 2012 by two cases of H10N7 infection among workers at a poultry slaughterhouse in Australia (Arzey et al., 2012). More recently, repeated human infections with H10 viruses have been reported in China. In 2014, Jiangxi Province confirmed the first human case caused by a novel reassortant H10N8 virus, marking the first known fatality associated with this subtype (To et al., 2014). In 2021, Jiangsu Province reported the first human infection with the novel H10N3 virus (Qi et al., 2022), and in 2022, Zhejiang Province confirmed the second case (Zhang et al., 2023). Both patients developed severe pneumonia but recovered after treatment. At the end of 2023, a co-infection involving the novel H10N5 virus and seasonal H3N2 influenza virus was reported in Zhejiang Province, representing the first global report of human infection with H10N5 (Yang et al., 2025). Furthermore, additional human infections with H10N3 were reported in Yunnan and Guangxi in 2024 and 2025 (Wang et al., 2025; WHO, 2025). These events demonstrate that the H10 subtype AIV carries the potential for human-to-human transmission and therefore warrants heightened vigilance.

Currently, numerous technologies are available for influenza virus detection. The hemagglutinin (HA) and hemagglutination inhibition (HI) assays are widely used to detect hemagglutinating activity in allantoic fluid collected from virus isolation and to identify subtype-specific antibodies; however, their sensitivity is relatively low (Comin et al., 2013). Enzyme-linked immunosorbent assays (ELISA) are also broadly employed. Double-antibody sandwich ELISA targeting the nucleoprotein of AIV (Zhang et al., 2006) and antigen-capture ELISA based on monoclonal antibodies specific for conformational or linear epitopes of viral HA and neuraminidase are both suitable for on-site or environmental testing (Ho et al., 2009). Compared with HA and HI, these ELISAs exhibit markedly higher sensitivity and specificity, but their inter-assay reproducibility is poor (Fu et al., 2023). Reverse-transcription polymerase chain reaction (RT-PCR) offers higher sensitivity than ELISA and greater efficiency than traditional virus isolation, but its performance can be compromised by PCR inhibitors, inefficient RNA extraction, and rapid RNA degradation (Chen et al., 2007). Colloidal gold immunochromatography is a simple and inexpensive lateral-flow assay that relies on antigen–antibody binding, but quantitative analysis remains difficult (Han et al., 2020). Other biosensor-based approaches, such as surface plasmon resonance and field-effect transistors, require high-quality samples and complex procedures, limiting their practical use (Li et al., 2021; Park et al., 2025).

Time-resolved fluorescence immunoassay (TRFIA) is distinguished by its use of fluorescent lanthanide chelate labels, providing much higher sensitivity than radioisotope-based methods and making it a powerful tool for ultra-trace analysis. TRFIA combines high specificity, rapid turnaround, cost-effectiveness, minimal matrix interference, and a wide dynamic range, and has been widely applied in the diagnosis of viral diseases in both humans and animals (Liu et al., 2023; Lu et al., 2025; Yuan and Wang, 2005).

The objective of this study was to develop and evaluate a time-resolved fluorescence immunochromatographic strip assay for the rapid detection of H10 subtype AIV. By pairing two monoclonal antibodies specific to the H10 HA protein, we constructed a highly sensitive and specific strip test suitable for field application. The analytical performance, diagnostic accuracy, and practical utility of this assay were assessed in comparison with established methods to determine its value for surveillance in poultry populations and live bird markets.

Materials and methods

Cells and viruses

The Madin–Darby canine kidney (MDCK) cell line (catalog no. CL-0043, Pricella Biotechnology Co., Ltd., Wuhan, China) was routinely cultured in Dulbecco's modified Eagle medium (DMEM; Gibco, Thermo Fisher Scientific, Waltham, MA, USA) supplemented with 10 % fetal bovine serum (FBS; Gibco). Field H10 isolates recovered from poultry farms in eastern China served as viral stocks. Both MDCK cells and viruses were stored at $-80°C$. For propagation, 9-day-old specific-pathogen-free (SPF) embryonated eggs (Beijing Merial Vital Laboratory Animal Technology Co., Ltd., Beijing, China) were inoculated and incubated at $37°C$; allantoic fluid was harvested 48 h post-inoculation. The HA protein of A/chicken/Zhejiang/2CP8/2014 (H10N7) was expressed and purified as previously described (Shen et al., 2017). Virus panels used in this study are listed in Table 1.

Generation of mAbs against H10 AIV

Five 6-week-old female BALB/c mice (Shanghai Laboratory Animal Center, Shanghai, China) were immunized intramuscularly with chromatographically purified H10N7 HA protein emulsified in Quick Antibody Adjuvant (catalog no. QAD1002, Biodragon Immunotechnologies, Suzhou, China). A booster was administered three weeks later. Tail-vein sera were screened by ELISA (SpectraMax i3x, Molecular Devices, San Jose, CA, USA) to quantify HA-specific IgG titers. Splenocytes from mice with the highest serological reactivity were harvested and fused with SP2/0 mouse myeloma cells (ATCC, Manassas, VA, USA) using polyethylene glycol (PEG 1500, Roche Diagnostics, Mannheim, Germany).

Table 1
The viruses mentioned in this study.

Virus subtype	Strain name	Virus titer
H1N2	A/duck/Zhejiang/D1/2013	2^6 HAU
H2N8	A/duck/Zhejiang/6D10/2013	2^7 HAU
H3N2	A/duck/Zhejiang/4613/2013	2^7 HAU
H4N2	A/duck/Zhejiang/727145/2014	2^6 HAU
H5N1	A/goose/Zhejiang/112071/2014	2^5 HAU
H6N1	A/chicken/Zhejiang/1664/2017	2^5 HAU
H7N9	A/chicken/Zhejiang/DTID-ZJU01/2013	2^7 HAU
H9N2	A/chicken/Zhejiang/329/2011	2^8 HAU
H10N2	A/duck/Zhejiang/6D20/2013	2^7 HAU
H10N3	A/chicken/Zhejiang/8615/2016	2^7 HAU
H10N3	A/chicken/Zhejiang/516100/2017	2^8 HAU
H10N3	A/Zhejiang/CDK/2022	2^6 HAU
H10N5	A/Zhejiang/CNIC-ZJU01/2023	2^5 HAU
H10N7	A/chicken/Zhejiang/2CP8/2014	2^5 HAU
H10N7	A/chicken/Zhejiang/528189/2016	2^6 HAU
H10N8	A/chicken/Zhejiang/121711/2016	2^5 HAU
H10N8	A/chicken/Zhejiang/102615/2016	2^5 HAU
H11N3	A/duck/Zhejiang/727D2/2013	2^8 HAU
Newcastle disease virus (NDV)	La Sota	10^5 EID50
Newcastle disease virus (NDV)	Clone 30	10^5 EID50
Infectious bronchitis virus (IBV)	H120	$10^{3.5}$ EID50
Infectious bronchitis virus (IBV)	H52	$10^{5.5}$ EID50
Infectious bursal disease virus (IBDV)	NF8	10^5 TCID50
Infectious bursal disease virus (IBDV)	B87	10^3 TCID50
Avian paramyxovirus-4 (APMV-4)	ZJ-1	10^6 EID50
Marek's disease virus (MDV)	FC-126	10^4 PFU
Infectious laryngotracheitis virus (ILTV)	K317	10^5 EID50
Avian pox virus (APV)	Quail-adapted strain	10^5 EID50

Hybridoma supernatants were screened by ELISA with recombinant HA protein passively adsorbed onto 96-well microplates (Corning Inc., Corning, NY, USA). Positive clones were purified using Protein G columns (GE Healthcare, Chicago, IL, USA). Antibody concentration was determined spectrophotometrically (NanoDrop 2000, Thermo Fisher Scientific). Isotypes were assigned with a mouse monoclonal antibody isotyping kit (Bio-Rad, Hercules, CA, USA).

Affinity of mAbs—indirect ELISA

To assess the affinity and binding activity of mAbs, 96-well plates were coated overnight at 4°C with 20 ng of urified H10N7 HA protein per well. On the following day, 100 μL of 0.1μg/mL mAbs were added to the first column of the plates that were pre-blocked, performed two-fold serial dilutions with PBS (pH 7.4; Sangon, Shanghai, China) and incubated at 37°C for 1 hour. After washing the plates, HRP-conjugated goat anti-mouse IgG (Novus Biologicals, Centennial, CO, USA) was applied and incubated at 37°C for 0.5 hour. Chromogenic development was initiated with TMB substrate and terminated with acidic stop solution, and absorbance was read at 450 nm on a SpectraMax plate reader (Molecular Devices, San Jose).

HI and microneutralization (MN) activity of mAbs

Prior to HI testing, viral stocks were standardized by endpoint titration with 1 % chicken erythrocytes (SPF chickens, Merial Vital, Beijing, China). mAbs were serially diluted in PBS and combined with virus suspension standardized to 4 hemagglutination units (HAU). After 30 min equilibration in V-bottom 96-well plates (Nunc, Thermo Fisher Scientific, Waltham, MA, USA), 1 % chicken red blood cells were added. The HI titer was recorded as the highest dilution completely inhibiting hemagglutination. For the MN assay, MDCK cells were seeded at 20000 cells/well in 96-well plates (Corning). Antibodies were serially diluted and incubated with 100 TCID50 of H10 virus for 2 h at 37°C, then transferred to MDCK cultures. Viral replication was assessed by HI assay, and neutralizing potency was calculated by the Reed–Muench method (Reed and Muench, 1938).

Immunofluorescence (IFA)

Subtype specificity of mAbs 2E3 and 2E9 was evaluated by IFA against a panel of AIV strains. MDCK cells were seeded into 48-well plates (Corning) and infected at a multiplicity of infection of 0.5. At 16 h post-infection, cells were fixed with 4 % paraformaldehyde (Sigma–Aldrich), permeabilized with 0.5 % Triton X-100 (Sigma–Aldrich), and blocked with 3 % bovine serum albumin (BSA; Sangon). Primary antibodies (10 μg/mL) were incubated overnight at 4°C. Alexa Fluor 488-conjugated goat anti-mouse IgG (Abcam, Cambridge, UK) was used as the secondary antibody. Nuclei were stained with DAPI (Beyotime, Shanghai, China). Fluorescence images were captured with an inverted fluorescence microscope (Olympus IX73, Olympus Corporation, Tokyo, Japan).

Development of the H10 TRFIA-ICS

Seventy microliters of Eu^{3+}-chelated fluorescent microspheres (200 nm, Thermo Fisher Scientific) were diluted into 500 μL of 25 mM 4-morpholineethanesulfonic acid (MES) buffer (Sigma–Aldrich). To activate surface carboxyl groups, 16 μL of freshly prepared 1-ethyl-3-(3-dimethylaminopropyl) carbodiimide hydrochloride (EDC; catalog no. 22980, Thermo Fisher Scientific) and an equal volume of N-hydroxysuccinimide (NHS; catalog no. 56480, Sigma–Aldrich) were added. The mixture was gently shaken on a horizontal vibrating platform in the dark for 15 min at ambient temperature. Excess coupling reagents were removed by ultracentrifugation (15,000 rpm, 10 min, 4°C; Beckman Coulter Optima, Brea, CA, USA). The pellet was resuspended in 400 μL of MES buffer

containing 0.2 mg of monoclonal antibody 2E3 and incubated for 1 h at room temperature. Unreacted sites were saturated by adding 400 μL of blocking solution (10 % BSA; Sangon) and incubating for another 1 h at room temperature. The conjugates were washed twice with phosphate-buffered saline containing 1 % Tween-20 (PBT; Sangon) to remove residual antibodies and reagents, after which they were collected by ultracentrifugation and resuspended in 120 μL of PBT.

Aliquots of the conjugate suspension were sprayed uniformly onto glass-fiber conjugate pads (Jiening Biotech, Shanghai, China) using a low-pressure airbrush (Iwata Eclipse, Anest Iwata Corp., Yokohama, Japan). Goat anti-mouse IgG (1 mg/mL; Solarbio Life Sciences, Beijing, China) and mAb 2E9 (4 mg/mL) were striped onto nitrocellulose membranes (Sartorius AG, Göttingen, Germany) as control (C) and test (T) lines, respectively, using a BioDot XYZ dispensing system (model XYZ3060, BioDot Inc., Irvine, CA, USA) set at 1 μL/cm. The time-resolved fluoroimmunoassay immunochromatographic strip (TRFIA-ICS) was then assembled in sequence with a sample pad, conjugate pad, nitrocellulose membrane, and absorbent pad, all mounted on an adhesive polyvinyl chloride (PVC) backing card (Jiening Biotech). After lamination, cards were cut into 3.5-mm-wide strips using an automated cutter (Jinbiao Biotech).

For testing, 80 μL of the sample was applied to the glass-fiber conjugate pad. Visual inspection was performed under 365-nm ultraviolet light (UVP LLC, Upland, CA, USA), and quantitative fluorescence intensities were recorded using a handheld strip reader (Hemai Technology, Suzhou, China). The fluorescence signal of PBS was set as the negative control, and signals higher than this threshold were defined as positive.

Performance evaluation of the H10 TRFIA-ICS

The specificity of the TRFIA–ICS was examined using a panel of avian influenza virus subtypes, H10N2, H10N3, H10N5, H10N7, H10N8, H1N2, H2N8, H3N2, H4N2, H5N1, H6N1, H7N9, H9N2, and H11N3, as well as several non-influenza avian pathogens, including avian paramyxovirus type 4 (APMV-4, strain ZJ-1), infectious bronchitis virus (IBV, strains H120 and H52), infectious bursal disease virus (IBDV, strains NF8 and B87), Newcastle disease virus (NDV, strains La Sota and Clone 30), Marek's disease virus (MDV, strain FC-126), infectious laryngotracheitis virus (ILTV, strain K317), and avian pox virus (APV, quail-adapted strain). Each viral allantoic fluid sample was diluted with PBS to 2^5 HAU, and PBS served as the negative control. Each diluted sample was applied to individual strips, and results were recorded both visually under UV light (UVP LLC, Upland, CA, USA) and quantitatively with a fluorescence strip reader (Hemai Technology, Suzhou, China).

For sensitivity testing, two-fold serial dilutions of allantoic fluid containing H10 AIV (starting at 2^5 HAU) and purified H10 HA protein (starting at 300 ng/mL) were tested on freshly prepared strips. Reproducibility was assessed by repeatedly assaying ($n = 35$) H10 AIV allantoic fluid diluted to 2^5, 2^3, 2^1, 2^{-1}, 2^{-3}, and 2^{-5} HAU. Fluorescence intensities were measured, and relative standard deviations (RSDs) were calculated for each concentration to assess variability.

For quantitative analysis, a linear regression model was established to describe the mathematical relationship between fluorescence signal intensity and sample concentration (GraphPad Prism 10, GraphPad Software, San Diego, CA, USA). Receiver operating characteristic (ROC) curve analysis was also conducted to evaluate diagnostic performance, and the area under the curve (AUC) was calculated.

Results

Characteristics of mAbs 2E3 and 2E9

Two rounds of immunization were performed on six-week-old BALB/c female mice, and sera were collected from the tail vein one week after the second immunization. Antibody titers were determined by ELISA,

and mice with higher titers were selected for intraperitoneal booster immunization three days prior to cell fusion. Spleen cells were harvested and fused with SP2/0 myeloma cells, and antibody secretion in culture supernatants was monitored weekly by ELISA. Clones exhibiting high antibody levels and monoclonality were subcloned and maintained through three successive passages. Stable clones were then expanded, and ascitic fluid was produced by intraperitoneal injection into BALB/c mice. Monoclonal antibodies were purified from ascites and designated as 2E3 and 2E9 (Fig. 1A).

Affinity analysis showed that the 2E3 antibody had an affinity of 4×10^{-4} µg/mL, while 2E9 exhibited an affinity of 8×10^{-4} µg/mL. Both antibodies specifically bound to the H10 subtype influenza virus but not to other influenza A subtypes (Fig. 2). HI and MN assays demonstrated that both antibodies exhibited strong inhibitory activity against H10 AIVs. HI titers were comparable between 2E3 and 2E9, while neutralization assays revealed that 2E3 had stronger activity than 2E9 against H10N2, H10N3, H10N7, and H10N8 viruses, but weaker activity against H10N5. The neutralizing potency of both 2E3 and 2E9 against H10N5 was reduced by 10- to >1,000-fold compared with other H10 subtypes (Table 2). Phylogenetic analysis showed that the H10N5 strain clustered separately from other H10 viruses (Fig. 3).

Limit of detection of the TRFIA-ICS

Serial two-fold dilutions of allantoic fluid containing H10 AIV were prepared and applied to the conjugate pads. After 15 min, strips were illuminated with 365-nm ultraviolet light, and fluorescence signals were quantified (Fig. 1B). Fluorescence intensities remained high from 2^5 to 2^1 HAU, but declined sharply between 2^0 and 2^{-1} HAU. Background readings from PBS averaged around 1,000 RFU; therefore, signals above 2,000 RFU were considered positive. Repeated testing established a detection limit of 0.015 HAU for the TRFIA-ICS. When purified HA protein was used, the detection limit was 1.1 ng/mL (Fig. 4).

Specificity of TRFIA-ICS

The assay was evaluated against multiple H10 subtypes (H10N2, H10N3, H10N5, H10N7, and H10N8) and consistently yielded positive results. In contrast, other avian influenza subtypes (H1N2, H2N8, H3N2, H4N2, H5N1, H6N1, H7N9, H9N2, and H11N3) and other common avian pathogens, including NDV, IBV, IBDV, APMV-4, MDV, ILTV, and APV, tested negative (Table 1; Fig. 5). These results demonstrated that the TRFIA-ICS exhibited high specificity without cross-reactivity.

Reproducibility, ROC curve, and linear regression analysis

Reproducibility was assessed by repeatedly testing H10 AIV allantoic fluid at six viral titers (2^5, 2^3, 2^1, 2^{-1}, 2^{-3}, and 2^{-5} HAU) with 35 replicates each. Fluorescence intensities were recorded and statistically analyzed. Across all concentrations, the relative standard deviation (RSD) remained below 10 % (Table 3), indicating stable repeatability and minimal variation between replicates.
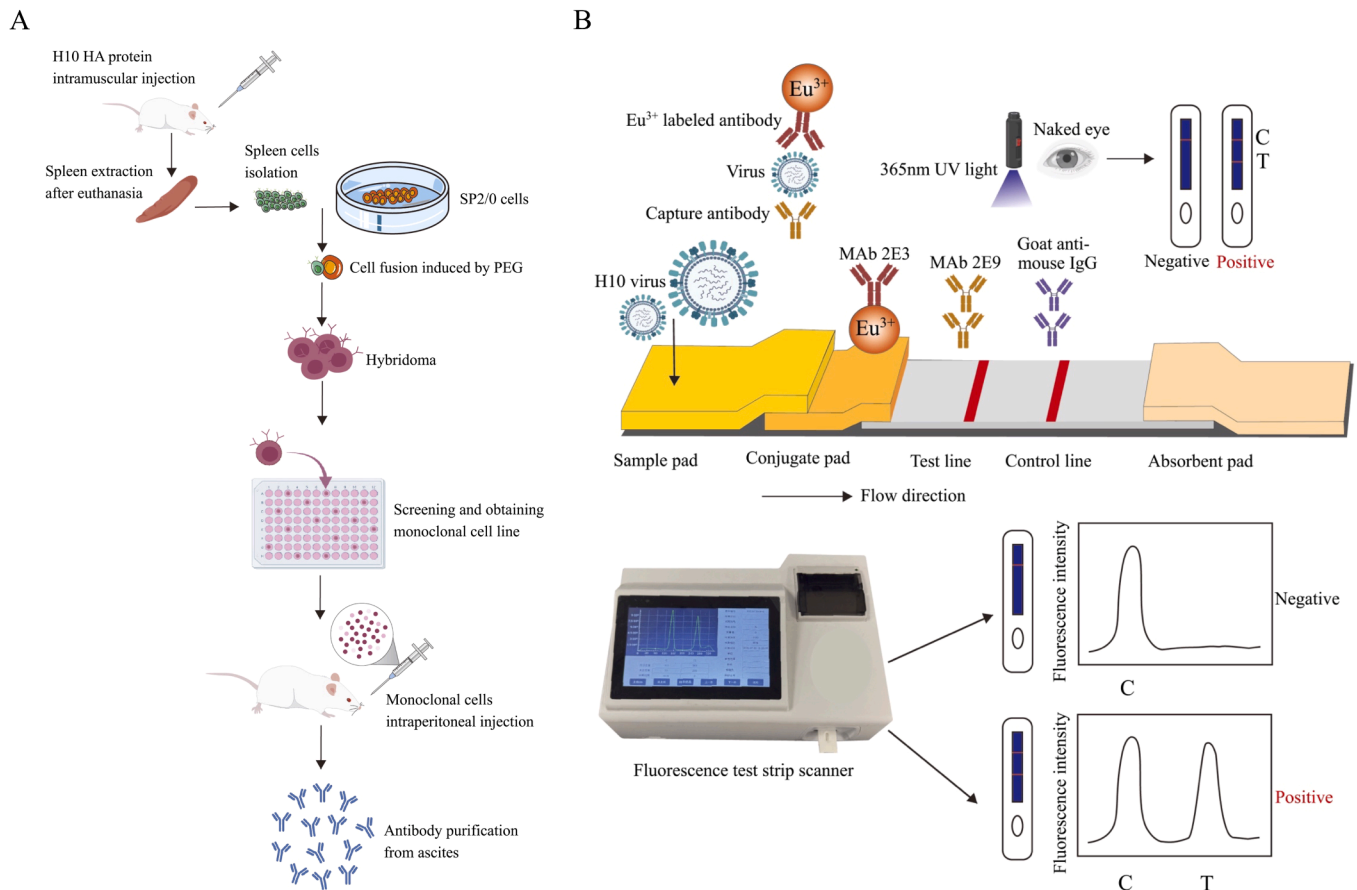

Fig. 1. Schematic illustration of mAb production and principle of the TRFIA-ICS for H10 AIV detection. (A) Procedure for generation of mAbs against H10 HA protein. Mice were immunized with H10 HA protein, splenocytes were fused with SP2/0 myeloma cells, and hybridomas secreting H10-specific mAbs were screened. Positive clones were expanded, injected intraperitoneally into mice, and antibodies were purified from ascitic fluid. (B) Principle of the TRFIA-ICS. Eu³⁺-labeled mAb 2E3 was used as a detection antibody, and mAb 2E9 was immobilized on the test line. Goat anti-mouse IgG was applied to the control line. In the presence of H10 virus, antigen–antibody complexes accumulated at the test line, producing a fluorescent signal visible under 365-nm UV light and quantifiable using a fluorescence strip reader. Negative and positive interpretations are shown by signal intensity at the control (C) and test (T) lines.
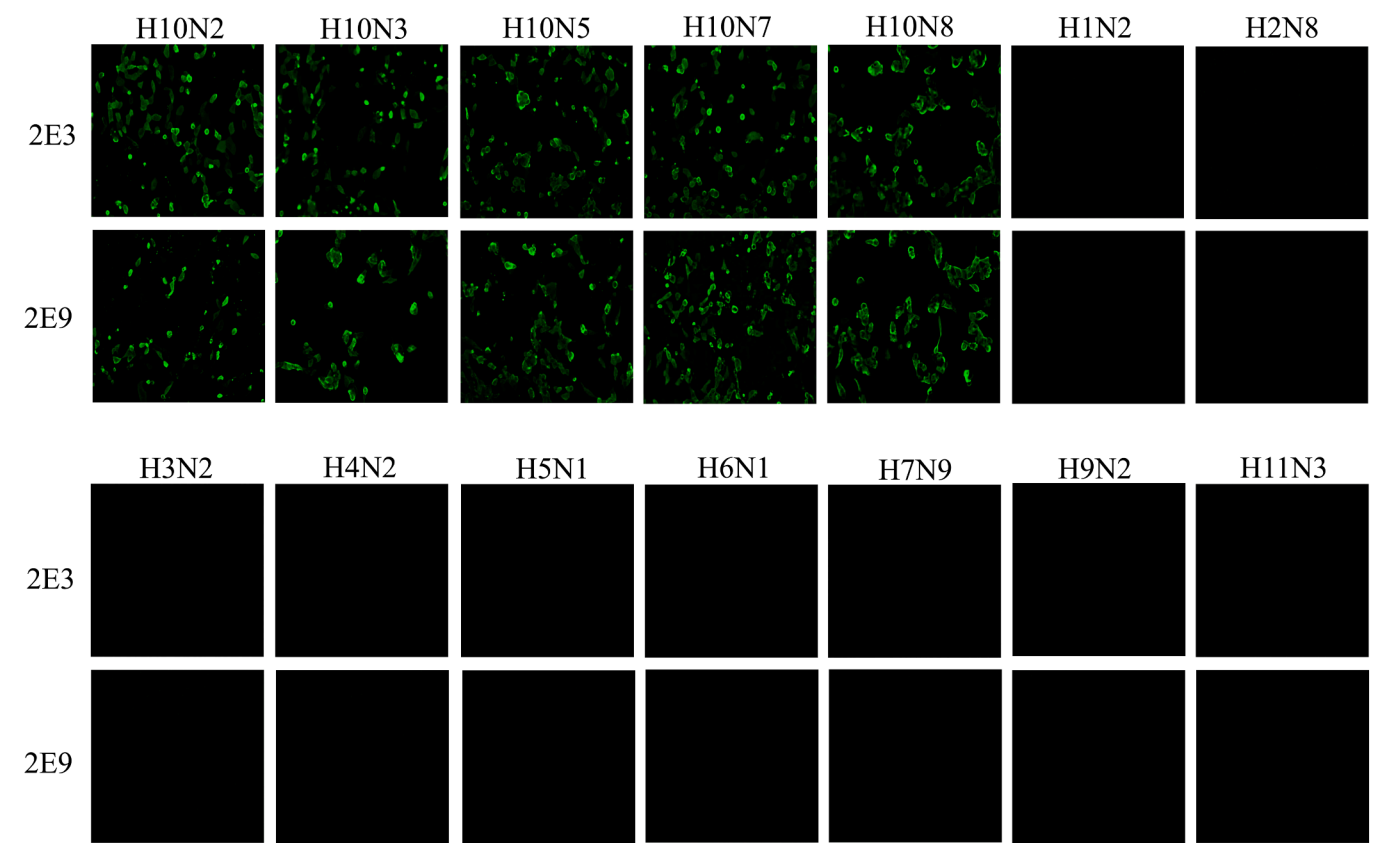
Fig. 2. Immunofluorescence assay demonstrating the binding specificity of mAbs 2E3 and 2E9 to H10 subtype AIVs. MDCK cells were infected with the indicated AIV subtypes (top row, left to right: H10N2, H10N3, H10N5, H10N7, H10N8, H1N2, H2N8; bottom row, left to right: H3N2, H4N2, H5N1, H6N1, H7N9, H9N2, H11N3). After fixation and permeabilization, cells were incubated with 2E3 or 2E9 (10 μg/mL) followed by Alexa Fluor 488–conjugated goat anti-mouse IgG. Green fluorescence indicates positive antibody binding. Both mAbs showed strong reactivity with H10 subtypes and no detectable binding to non-H10 subtypes (representative fields shown).

Table 2
Characterization of monoclonal antibodies (mAbs) against H10 subtype avian influenza viruses.

Name	Affinity	Isotype		H10N2		H10N3		H10N5		H10N7		H10N8	
	(μg/mL)	Subclass	Type	HI titer (μg/mL)	MN titer (ng/mL)	HI titer (μg/mL)	MN titer (ng/mL)	HI titer (μg/mL)	MN titer (ng/mL)	HI titer (μg/mL)	MN titer (ng/mL)	HI titer (μg/mL)	MN titer (ng/mL)
2E3	4×10^{-4}	IgG2a	κ	0.78	97.65	3.12	195.31	31.25	250000.00	1.56	390.62	6.25	390.62
2E9	8×10^{-4}	IgG2b	κ	1.56	97.65	6.25	12500.00	62.50	125000.00	1.56	1562.50	6.25	781.25

The affinity of the mAbs was evaluated using ELISA. The concentration of coated purified HA protein started at 0.1 μg/mL. Each mAb was subjected to successive two-fold dilutions in PBS, followed by identical ELISA processing.

The isotypes of the monoclonal antibodies were determined using a mouse monoclonal antibody isotyping kit (Bio-Rad, Hercules, CA, USA). Type indicates the light chain type of mAb.

The H10 viruses used for HI and MN assays were as follows: H10N2 (A/duck/Zhejiang/6D20/2013), H10N3 (A/chicken/Zhejiang/8615/2016), H10N5 (A/Zhejiang/CNIC-ZJU01/2023), H10N7 (A/chicken/Zhejiang/2CP8/2014), and H10N8 (A/chicken/Zhejiang/121711/2016). The initial concentration of these mAbs was 20 μg/mL for HI and 1000 μg/mL for MN.

ROC curve analysis of the assay showed an area under the curve (AUC) of 0.9896 for virus-containing allantoic fluid and 0.9722 for purified HA protein. These results confirmed that the assay could reliably distinguish positive from negative samples with a very low probability of false-positive results. Linear regression analysis demonstrated a strong linear relationship between fluorescence signal intensity and either virus titer or protein concentration, enabling accurate quantitative prediction (Fig. 6).

Evaluation of the TRFIA-ICS with field samples

The TRFIA-ICS was further evaluated using 174 avian-origin samples, including cloacal swabs, throat swabs, and fecal samples. Among these, 31 samples tested positive for H10 AIV. The same panel of samples was also examined by real-time PCR, which served as the gold standard. All samples showed identical classifications between TRFIA-ICS and real-time PCR, resulting in a 100 % concordance rate (Table 4). These findings confirmed that the TRFIA-ICS maintained high sensitivity and specificity when applied to field specimens.

Discussion

With the increasing frequency of human infections by H10 subtype AIVs in recent years, the development of highly sensitive and specific diagnostic methods is of urgent importance for monitoring and control. Traditional methods such as the HI assay have been widely applied for
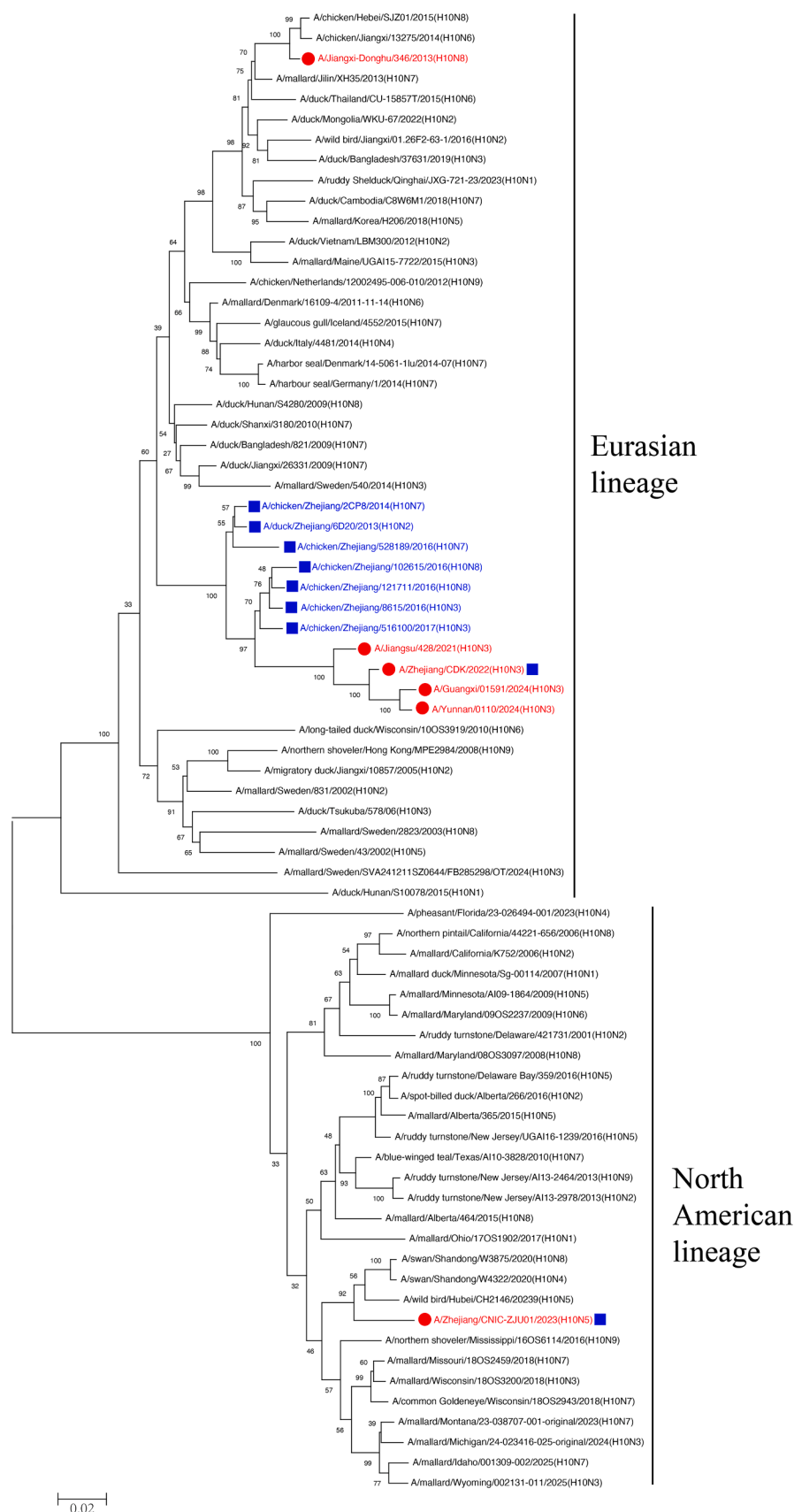
Fig. 3. Phylogenetic analysis of *HA* genes of H10 subtype viruses. An evolutionary tree was constructed to show the genetic relationships of H10 subtype virus strains. Information on representative H10 subtype viruses' *HA* gene sequences was downloaded from the National Center for Biotechnology Information database and GISAID. The evolutionary tree was generated using the MEGA11 version. The H10 subtype strains used in this study are highlighted with blue frames. H10 subtype strains that have infected humans are indicated with red circles.
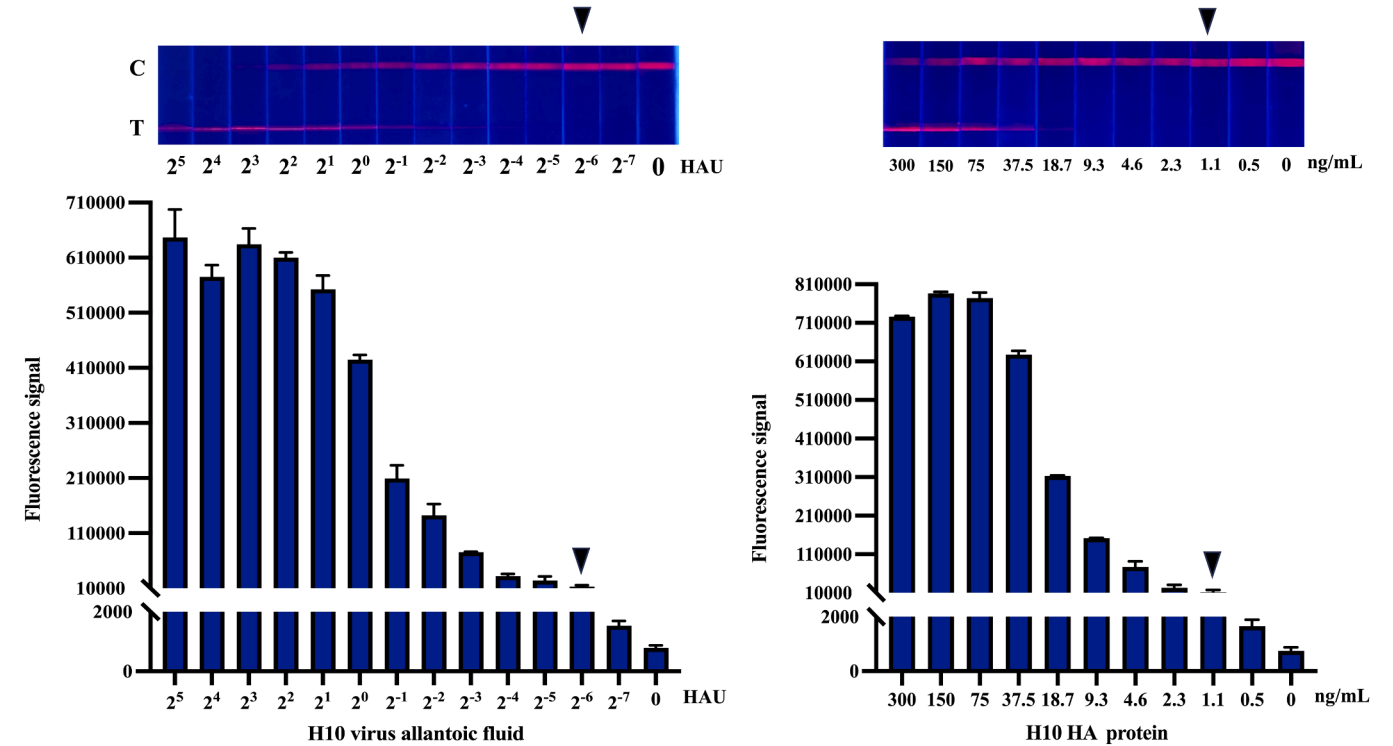
Fig. 4. Detection sensitivity of the TRFIA-ICS under 365-nm ultraviolet excitation. (A) Serial two-fold dilutions of H10N7 AIV, ranging from 2^5 to 2^{-7} HAU, were tested to determine the detection limit of the TRFIA-ICS. Representative test strips and corresponding fluorescence intensity scans recorded by the fluorescence strip scanner are shown. (B) Serial dilutions of purified H10N7 HA protein, ranging from 300 to 0.5 ng/mL, were used to determine the detection limit of the TRFIA-ICS. Representative test strips and fluorescence intensity scans measured by the fluorescence strip scanner are shown.
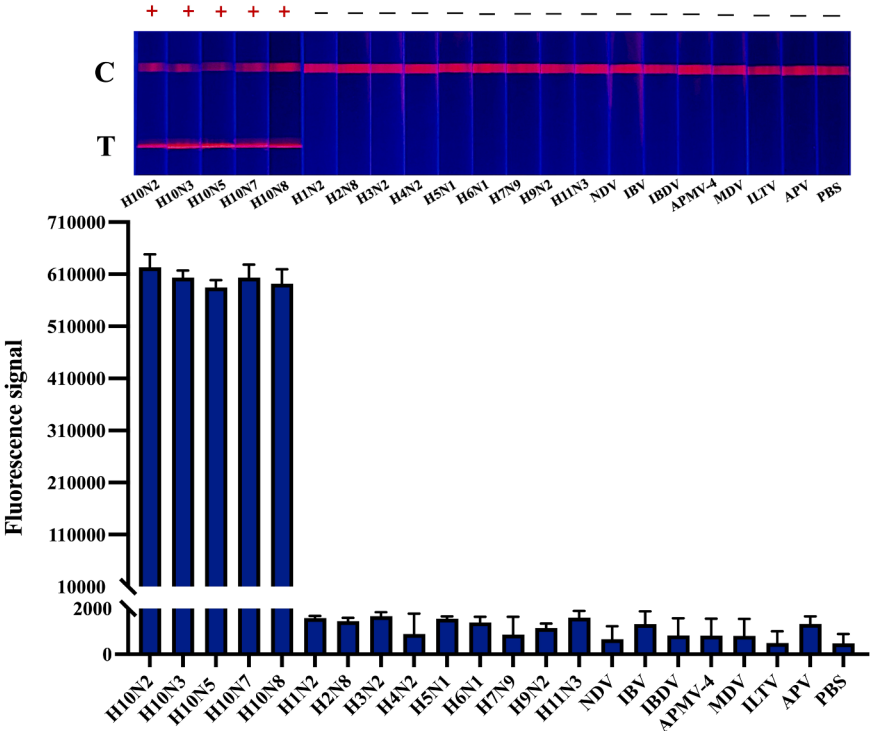

Fig. 5. Cross-reactivity analysis of the TRFIA-ICS. The assay was tested against multiple influenza A virus subtypes (H10N2, H10N3, H10N5, H10N7, H10N8, H1N2, H2N8, H3N2, H4N2, H5N1, H6N1, H7N9, H9N2, and H11N3) as well as other avian respiratory tract viruses, including Newcastle disease virus (NDV), infectious bronchitis virus (IBV), infectious bursal disease virus (IBDV), avian paramyxovirus type 4 (APMV-4), Marek's disease virus (MDV), infectious laryngotracheitis virus (ILTV), and avian pox virus (APV).

Table 3
Reproducibility of H10 TRFIA-ICS.

Virus concentration (HAU)	Fluorescence signal average	Std. dev	CV (%)
2^5	627909	44276.5	7.05
2^3	595280	33784.8	5.67
2^1	555486	29513.4	5.31
2^{-1}	254516	22778.2	8.94
2^{-3}	83046	6491.7	7.81
2^{-5}	24003	2327.0	9.69

Abbreviations: HAU, hemagglutination units; TRFIA-ICS, time-resolved fluorescence immunoassay–immunochromatographic strip; Std. dev., standard deviation; CV, Coefficient of Variation.

influenza diagnosis, but their sensitivity is low and they are influenced by erythrocyte type and quality. Furthermore, cross-reactivity among influenza viruses often reduces diagnostic specificity, limiting their diagnostic utility (Stephenson et al., 2003; Tavakoli et al., 2017).

ELISA-based techniques, including DAS-ELISA and AC-ELISA, have improved detection limits for AIVs. For example, the detection limit for H10N8 and H7N9 AIVs ranges from 0.5 to 2 HAU, while purified HA protein can typically be detected at concentrations of 1–5 µg/mL (Chen et al., 2019; Yu et al., 2019). Despite these advantages, ELISAs are limited by inter-batch variation in coating efficiency and enzymatic activity, which may compromise reproducibility. Similarly, the colloidal gold ICS developed for H7N9 and H9N2 detection showed detection limits of 2 HAU and 4 HAU, respectively, but quantitative analysis is not easily achieved with colloidal gold (Yang et al., 2020a; Xiao et al., 2021).

To address these limitations, TRFIA-based methods have been explored due to their high sensitivity, wide dynamic range, and strong reproducibility. In previous work, a quantum-dot ICS developed for H10 AIV achieved a detection limit of 0.125 HAU for virus-containing allantoic fluid and 4 ng/mL for purified HA protein (Fu et al., 2025). In the present study, the TRFIA-ICS lowered the detection limit further to 0.015 HAU for allantoic fluid and 1.1 ng/mL for purified HA protein, confirming superior sensitivity. These improvements were achieved by combining Eu^{3+}-chelate with two monoclonal antibodies targeting the HA protein, which enhanced signal stability and reduced background noise.

Table 4
Comparison of the results of the TRFIA-ICS and Real-time PCR for 174 poultry samples.

		Real-time PCR		
		Negative	Positive	Total
TRFIA-ICS	Negative	158	0	158
	Positive	0	16	16
	Total	158	16	174
Overall coincidence rate				100 %

Abbreviations: Real-time PCR, real-time polymerase chain reaction; TRFIA-ICS, time-resolved fluorescence immunoassay–immunochromatographic strip.
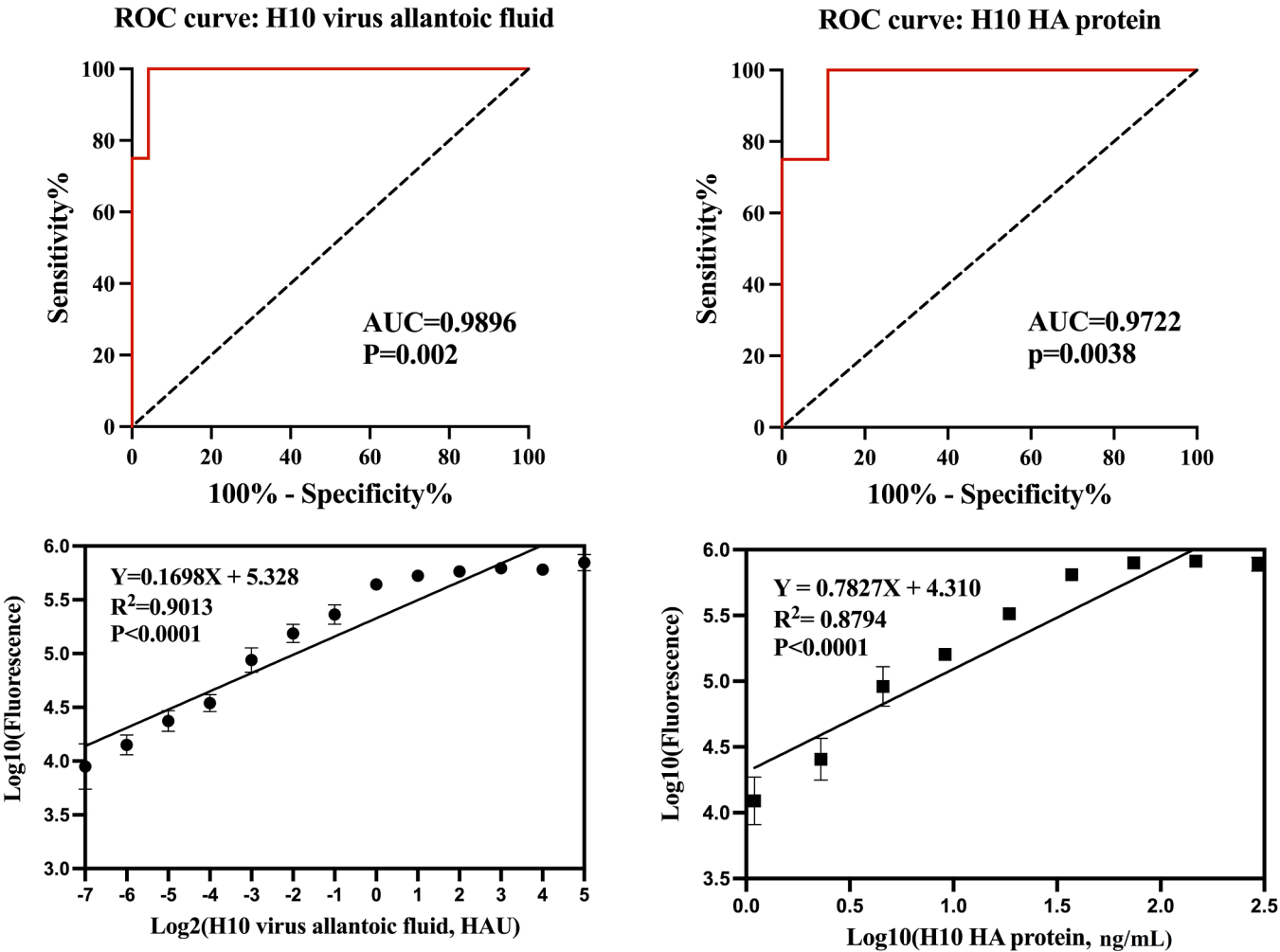

Fig. 6. Receiver operating characteristic (ROC) curve and linear regression analysis of the TRFIA-ICS. ROC curves and regression analyses were generated using GraphPad Prism 10 (GraphPad Software, San Diego, CA, USA).

The specificity of the TRFIA-ICS was also outstanding. It successfully identified all tested H10 subtypes, including H10N2, H10N3, H10N5, H10N7, and H10N8, without cross-reactivity to nine other AIV subtypes or seven common avian pathogens. Such specificity is particularly important for field applications, where mixed infections or environmental contaminants can interfere with detection. The high reproducibility of the assay was confirmed by relative standard deviation values below 10 % across multiple concentrations, underscoring its reliability for repeated use.

Quantitative analysis was another key feature of this assay. ROC curve analysis demonstrated near-perfect discrimination between positive and negative samples, with AUC values of 0.9896 (HAU-based) and 0.9722 (HA protein-based). Linear regression revealed a strong correlation between fluorescence signal and virus concentration, enabling accurate quantitative evaluation of viral load. This capability represents a significant advantage over conventional ICS formats, which are primarily qualitative.

Importantly, the TRFIA-ICS performed well under field conditions. In 174 poultry-origin samples, including cloacal swabs, throat swabs, and fecal samples, the assay achieved complete concordance with RT-PCR. This finding indicates that the assay not only matches the sensitivity of the molecular gold standard but also provides results in only 15 min, with minimal technical requirements. These characteristics make it particularly suited for application in poultry farms, live bird markets, and other field settings where rapid and reliable diagnosis is essential for disease surveillance and control.

Conclusion

In conclusion, this study demonstrates that the TRFIA-ICS is a rapid, sensitive, specific, and reproducible tool for detecting H10 subtype AIVs. Compared with existing diagnostic assays, it significantly improves sensitivity and reproducibility while offering the convenience of a lateral-flow format. Its successful validation with field samples highlights its potential as a practical tool for large-scale surveillance of H10 AIVs in poultry populations, thereby contributing to early detection, prevention of spread, and protection of both animal and human health.

Declaration of AI

AI was not used to automatically generate the manuscript during the article writing process.

Ethics statement

The study was approved by the Animal Ethics Committee of the First Affiliated Hospital, School of Medicine, Zhejiang University (Approval No. 2024-35).

Data availability statement

The data that support the findings of this study are available from the corresponding author upon reasonable request.

CRediT authorship contribution statement

Ping Wang: Writing – original draft, Software, Data curation, Conceptualization. **Han Wu:** Writing – original draft, Software, Methodology, Formal analysis, Data curation. **Jiamin Fu:** Validation, Investigation, Formal analysis. **Jun Zhang:** Visualization, Validation, Software, Data curation. **Linfang Cheng:** Software, Resources, Investigation. **Fumin Liu:** Software, Methodology. **Hangping Yao:** Visualization, Supervision, Investigation. **Nanping Wu:** Supervision, Resources. **Haibo Wu:** Writing – review & editing, Supervision, Resources, Project administration, Funding acquisition, Conceptualization.

Disclosures

The authors declare that they have no known competing financial interests or personal relationships that could have appeared to influence the work reported in this paper.

References

Arzey, G.G., Kirkland, P..D., Arzey, K.E., Frost, M., Maywood, P., Conaty, S., Hurt, A.C., Deng, Y.M., Iannello, P., Barr, I., Dwyer, D.E., Ratnamohan, M., McPhie, K., Selleck, P., 2012. Influenza virus A (H10N7) in chickens and poultry abattoir workers, Australia. Emerg. Infect. Dis. 18, 814–816. https://doi.org/10.3201/eid1805.111852.

Bi, Y., Yang, J., Wang, L., Ran, L., Gao, G.F., 2024. Ecology and evolution of avian influenza viruses. Curr. Biol. 34, R716–r721. https://doi.org/10.1016/j.cub.2024.05.053.

Chen, L., Ruan, F., Liu, M., Zhou, J., Song, W., Qin, K., 2019. A sandwich ELISA for detecting the hemagglutinin of avian influenza A (H10N8) virus. J. Med. Virol. 91, 877–880. https://doi.org/10.1002/jmv.25387.

Chen, W., He, B., Li, C., Zhang, X., Wu, W., Yin, X., Fan, B., Fan, X., Wang, J., 2007. Real-time RT-PCR for H5N1 avian influenza A virus detection. J. Med. Microbiol. 56, 603–607. https://doi.org/10.1099/jmm.0.47014-0.

Comin, A., Toft, N., Stegeman, A., Klinkenberg, D., Marangon, S., 2013. Serological diagnosis of avian influenza in poultry: is the haemagglutination inhibition test really the 'gold standard'? Influenza Other Respir. Viruses 7, 257–264. https://doi.org/10.1111/j.1750-2659.2012.00391.x.

Fu, J., Wang, P., Cheng, L., Yan, S., Wu, H., Lu, X., Liu, F., Yao, H., Wu, N., Wu, H., 2025. Rapid and sensitive quantum dots immunochromatographic strip for H10 subtype Avian influenza virus detection. Transbound. Emerg. Dis. 2025, 6289957. https://doi.org/10.1155/tbed/6289957.

Fu, X., Wang, Q., Ma, B., Zhang, B., Sun, K., Yu, X., Ye, Z., Zhang, M., 2023. Advances in detection techniques for the H5N1 Avian influenza virus. Int. J. Mol. Sci. 24, 17157. https://doi.org/10.3390/ijms242417157.

Han, M.Y., Xie, T..A., Li, J.X., Chen, H.J., Yang, X.H., Guo, X.G., 2020. Evaluation of lateral-flow assay for rapid detection of influenza virus. Biomed. Res. Int. 2020, 3969868. https://doi.org/10.1155/2020/3969868.

Herfst, S., Zhang, J., Richard, M., McBride, R., Lexmond, P., Bestebroer, T.M., Spronken, M.I.J., de Meulder, D., van den Brand, J.M., Rosu, M.E., Martin, S.R., Gamblin, S.J., Xiong, X., Peng, W., Bodewes, R., van der Vries, E., Osterhaus, A., Paulson, J.C., Skehel, J.J., Fouchier, R.A.M., 2020. Hemagglutinin traits determine transmission of Avian A/H10N7 influenza virus between mammals. Cell Host Microbe 28. https://doi.org/10.1016/j.chom.2020.08.011, 602-613.e607.

Ho, H.T., Qian, H..L., He, F., Meng, T., Szyporta, M., Prabhu, N., Prabakaran, M., Chan, K.P., Kwang, J., 2009. Rapid detection of H5N1 subtype influenza viruses by antigen capture enzyme-linked immunosorbent assay using H5- and N1-specific monoclonal antibodies. Clin. Vaccine Immunol. 16, 726–732. https://doi.org/10.1128/cvi.00465-08.

Kang, M., Wang, L.F., Sun, B.W., Wan, W.B., Ji, X., Baele, G., Bi, Y.H., Suchard, M.A., Lai, A., Zhang, M., Wang, L., Zhu, Y.H., Ma, L., Li, H.P., Haerheng, A., Qi, Y.R., Wang, R.L., He, N., Su, S., 2024. Zoonotic infections by avian influenza virus: changing global epidemiology, investigation, and control. Lancet Infect. Dis. 24, e522–e531. https://doi.org/10.1016/s1473-3099(24)00234-2.

Krog, J.S., Hansen, M..S., Holm, E., Hjulsager, C.K., Chriél, M., Pedersen, K., Andresen, L.O., Abildstrøm, M., Jensen, T.H., Larsen, L.E., 2015. Influenza A(H10N7) virus in dead harbor seals, Denmark. Emerg. Infect. Dis. 21, 684–687. https://doi.org/10.3201/eid2104.141484.

Li, Y., Peng, Z., Holl, N.J., Hassan, M.R., Pappas, J.M., Wei, C., Izadi, O.H., Wang, Y., Dong, X., Wang, C., Huang, Y.W., Kim, D., Wu, C., 2021. MXene-graphene field-effect transistor sensing of influenza virus and SARS-CoV-2. ACS Omega 6, 6643–6653. https://doi.org/10.1021/acsomega.0c05421.

Liu, S., Ji, K., Chen, J., Tai, D., Jiang, W., Hou, G., Chen, J., Li, J., Huang, B., 2009. Panorama phylogenetic diversity and distribution of type A influenza virus. PLoS One 4, e5022. https://doi.org/10.1371/journal.pone.0005022.

Liu, T., Gao, C., Wang, J., Song, J., Chen, X., Chen, H., Zhao, X., Tang, H., Gu, D., 2023. Peptide aptamer-based time-resolved fluoroimmunoassay for CHIKV diagnosis. Virol. J. 20, 166. https://doi.org/10.1186/s12985-023-02132-w.

Lu, Z., Niu, J., Li, Y., Li, Y., Feng, D., Xu, S., Wang, L., 2025. Cascade signal amplification of time-resolved fluorescence immunoassay through enzyme catalysis coupled with dissolution enhancement. Anal. Chem. 97, 12306–12312. https://doi.org/10.1021/acs.analchem.5c01356.

Park, S., Lee, S., Park, J., Haam, S., Hwang, J., 2025. Tuning the aggregation of plasmonic probes to shed light on diagnostic strategies. ACS Sens. 10, 4083–4094. https://doi.org/10.1021/acssensors.5c00113.

Postel, A., Gremmel, N., Lydersen, C., Kovacs, K.M., Schick, L.A., Siebert, U., Nymo, I.H., Becher, P., 2025. Highly pathogenic avian influenza virus (H5N5) detected in an Atlantic walrus (Odobenus rosmarus rosmarus) in the Svalbard Archipelago, Norway, 2023. Emerg. Microbes Infect. 14, 2456146. https://doi.org/10.1080/22221751.2025.2456146.

Qi, X., Qiu, H., Hao, S., Zhu, F., Huang, Y., Xu, K., Yu, H., Wang, D., Zhou, L., Dai, Q., Zhou, Y., Wang, S., Huang, H., Yu, S., Huo, X., Chen, K., Liu, J., Hu, J., Wu, M., Bao, C., 2022. Human infection with an Avian-origin influenza A (H10N3) virus. N. Engl. J. Med. 386, 1087–1088. https://doi.org/10.1056/NEJMc2112416.

REED, L.J., MUENCH, H., 1938. A simple method of estimating fifty per cent Endpoints12. Am. J. Epidemiol. 27, 493–497. https://doi.org/10.1093/oxfordjournals.aje.a118408.

Shen, C., Chen, J., Li, R., Zhang, M., Wang, G., Stegalkina, S., Zhang, L., Chen, J., Cao, J., Bi, X., Anderson, S.F., Alefantis, T., Zhang, M., Cai, X., Yang, K., Zheng, Q., Fang, M., Yu, H., Luo, W., Zheng, Z., Yuan, Q., Zhang, J., Wai-Kuo Shih, J., Kleanthous, H., Chen, H., Chen, Y., Xia, N., 2017. A multimechanistic antibody targeting the receptor binding site potently cross-protects against influenza B viruses. Sci. Transl. Med. 9, eaam5752. https://doi.org/10.1126/scitranslmed.aam5752.

Stephenson, I., Wood, J.M., Nicholson, K.G., Zambon, M.C., 2003. Sialic acid receptor specificity on erythrocytes affects detection of antibody to avian influenza haemagglutinin. J. Med. Virol. 70, 391–398. https://doi.org/10.1002/jmv.10408.

Su, S., Qi, W., Zhou, P., Xiao, C., Yan, Z., Cui, J., Jia, K., Zhang, G., Gray, G.C., Liao, M., Li, S., 2014. First evidence of H10N8 avian influenza virus infections among feral dogs in live poultry markets in Guangdong province, China. Clin. Infect. Dis. 59, 748–750. https://doi.org/10.1093/cid/ciu345.

Tavakoli, A., Rezaei, F., Fatemi Nasab, G.S., Adjaminezhad-Fard, F., Noroozbabaei, Z., Mokhtari-Azad, T., 2017. The comparison of sensitivity and specificity of ELISA-based microneutralization test with hemagglutination inhibition test to evaluate neutralizing antibody against influenza virus (H1N1). Iran. J. Public Health 46, 1690–1696.

To, K.K., Tsang, A..K., Chan, J.F., Cheng, V.C., Chen, H., Yuen, K.Y., 2014. Emergence in China of human disease due to avian influenza A(H10N8)–cause for concern? J. Infect. 68, 205–215. https://doi.org/10.1016/j.jinf.2013.12.014.

Wang, X., Yu, H., Ma, Y., Zhang, P., Wang, X., Liang, J., Zhang, X., Gao, R., Lu, X., Yang, W., Chen, Y., Gu, M., Hu, J., Liu, X., Hu, S., Peng, D., Qi, X., Bao, C., Liu, K., Liu, X., 2025. The novel H10N3 avian influenza virus acquired airborne transmission

among chickens: an increasing threat to public health. mBio 16, e0236324. https://doi.org/10.1128/mbio.02363-24.

WHO 2025. Influenza at the human-animal interface summary and assessment. https://www.who.int 1 July 2025.

Xiao, Y., Yang, F., Liu, F., Yao, H., Wu, N., Wu, H., 2021. Antigen-capture ELISA and immunochromatographic test strip to detect the H9N2 subtype avian influenza virus rapidly based on monoclonal antibodies. Virol. J. 18, 198. https://doi.org/10.1186/s12985-021-01671-4.

Yang, F., Xiao, Y., Chen, B., Wang, L., Liu, F., Yao, H., Wu, N., Wu, H., 2020. Development of a colloidal gold-based immunochromatographic strip test using two monoclonal antibodies to detect H7N9 avian influenza virus. Virus Genes 56, 396–400. https://doi.org/10.1007/s11262-020-01742-8.

Yang, J., Zheng, S., Sun, J., Wu, H., Zhang, D., Wang, Y., Tian, T., Zhu, L., Wu, Z., Li, L., Gao, G.F., Bi, Y., Yao, H., 2025. A human-infecting H10N5 avian influenza virus: clinical features, virus reassortment, receptor-binding affinity, and possible transmission routes. J. Infect. 90, 106456. https://doi.org/10.1016/j.jinf.2025.106456.

Yu, D., Xiang, G., Zhu, W., Lei, X., Li, B., Meng, Y., Yang, L., Jiao, H., Li, X., Huang, W., Wei, H., Zhang, Y., Hai, Y., Zhang, H., Yue, H., Zou, S., Zhao, X., Li, C., Ao, D., Zhang, Y., Tan, M., Liu, J., Zhang, X., Gao, G.F., Meng, L., Wang, D., 2019. The re-emergence of highly pathogenic avian influenza H7N9 viruses in humans in mainland China, 2019. Euro Surveill. 24, 1900273. https://doi.org/10.2807/1560-7917.Es.2019.24.21.1900273.

Yuan, J., Wang, G., 2005. Lanthanide complex-based fluorescence label for time-resolved fluorescence bioassay. J. Fluoresc. 15, 559–568. https://doi.org/10.1007/s10895-005-2829-3.

Zhang, A., Jin, M., Liu, F., Guo, X., Hu, Q., Han, L., Tan, Y., Chen, H., 2006. Development and evaluation of a DAS-ELISA for rapid detection of avian influenza viruses. Avian Dis. 50, 325–330. https://doi.org/10.1637/7473-111605r.1.

Zhang, W., Zhang, Z., Wang, M., Pan, X., Jiang, X., 2023. Second identified human infection with the avian influenza virus H10N3: a case report. Ann. Intern. Med. 176, 429–431. https://doi.org/10.7326/l22-0376.

Zohari, S., Neimanis, A., Härkönen, T., Moraeus, C., Valarcher, J.F., 2014. Avian influenza A(H10N7) virus involvement in mass mortality of harbour seals (Phoca vitulina) in Sweden, March through October 2014. Euro Surveill. 19, 20967. https://doi.org/10.2807/1560-7917.es2014.19.46.20967.